ACS OMEGA

http://pubs.acs.org/journal/acsodf

Article

Tunable Radio Frequency Antenna Based on Phase Change Materials

Wei Wang, Wenxin Zeng, and Sameer R. Sonkusale*

Cite This: *ACS Omega* 2023, 8, 14665−14671

Read Online

ACCESS | Metrics & More | Article Recommendations

ABSTRACT: In conventional communication systems, dedicated tunable circuit elements are used to realize different functions and achieve performance metrics. For example, tuning the center frequency or the input impedance of an antenna in a radio frequency (RF) system is performed by complex impedance-matching circuits. In this paper, the antenna utilizes the temperature-induced irreversible mechanical deformation of a shape memory alloy (SMA) as a natural way to tune the antenna's shape and configuration, thereby providing inherent tunability without bulky circuit elements. This paradigm of material programming for impedance tuning of an SMA-based antenna is validated by both numerical simulation and measurements.

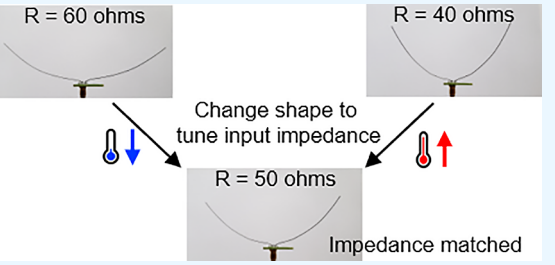

INTRODUCTION

Wireless communication over a radio frequency band such as using mobile phones has been the key technological innovation of the last half-century. To accommodate the need for an increasing user base, the electromagnetic spectrum is being reallocated and efficiently reutilized to support multiple users, using innovations in antenna design and architecture (e.g., multi-input multi-output (MIMO)), modulation schemes, and network architecture (e.g., GSM, CDMA, and LTE). There is a growing trend toward implementing programmable radios to support multiple communication protocols over multiple frequency bands. Programming the function and performance of an antenna system is typically achieved through dedicated tunable circuit components that are controlled using dedicated circuitry. For example, PN junction diodes switches have been widely used to tune antennas.[1−3] The parasitic capacitance of the PN junction diodes limits their efficacy. Additionally, the use of PN junction diodes and the tuning circuits consume electrical power, which requires a battery as the power supply. Microelectromechanical systems (MEMS) switches have also become another approach to tuning antennas.[4,5] However, MEMS have a high cost and short lifetime.

Antennas are radiating structures that emit or receive radio signals and are almost always fixed to support a given frequency band or mode of wireless communication. Here, we explored whether the material choices of the antenna can be used to tune antenna response without any electronic circuit elements. Conventional materials used in antennas are metals such as copper or iron. The shapes of these antennas are fixed and, therefore, only suitable for specific and fixed frequency signals. Flexible materials such as thread[6−9] and paper,[10−12] which can be made conductive through materials such as silver, have previously been used to realize various configurable antennas. Liquid metal-based antennas exhibiting easy reconfiguration have also been reported.[13−15] However, a capsule or microfluidic shell is needed to contain the liquid metal, which makes it more challenging to use in practice and can impact the electromagnetic (EM) performance of the antenna.

Such reconfigurable antennas have been demonstrated in the past for different frequency bands[16−19] and achieved varying radiation patterns.[20−23] However, these reconfigurability functions rely on extra devices, which increases the complexity and cost of the whole platform. Furthermore, the input impedance of the antennas is predetermined by their design, and an impedance-matching network is required to achieve the best performance. Rather than using extra devices to achieve reconfigurability, our group recently reported on using phase-changing materials such as shape memory alloys (SMAs) for antenna design. SMAs can achieve reconfigurable shapes by varying the temperature applied to the antenna. This phase changing memory behavior has been utilized in wireless temperature sensors where the antenna shape can record the temperature extrema.[24−26] In this article, a new approach is proposed for antenna reconfiguration through thermal programming of the underlying SMA rather than dedicated circuit elements. Temperature change causes the shape of the antenna

Received: January 27, 2023
Accepted: March 30, 2023
Published: April 11, 2023

https://doi.org/10.1021/acsomega.3c00550
ACS Omega 2023, 8, 14665−14671

to change in order to tune the input impedance of the antenna. In this way, there is no need for an extra matching circuit, since the input impedance of the antenna can directly match the port by itself. A dipole antenna was tested for proof of concept. However, the approach can be applied to other antenna configurations in the future.

MATERIALS AND METHODS

Thermomechanical Behavior of SMAs. SMAs are metal alloys with intrinsic thermomechanical memory that can monotonically transform from one predefined configuration to another depending on its initial configuration (shape) and the applied temperature profile. Through thermal training, two-way memory effect SMAs can switch between two crystal structures (austenite and detwinned martensite) at well-defined temperatures without any external stress.[24] As the temperature increases, the SMA transforms from a detwinned martensite phase to an austenite phase. The SMA can be transformed back to the detwinned martensite phase by reducing the temperature to the original starting temperature.[27] The critical start and end temperature for the formation of the martensite phase are defined as M_s and M_f, respectively, and the critical start and end temperature for the formation of an austenite phase are defined as A_s and A_f, as indicated in Figure 1. If the temperature is initially

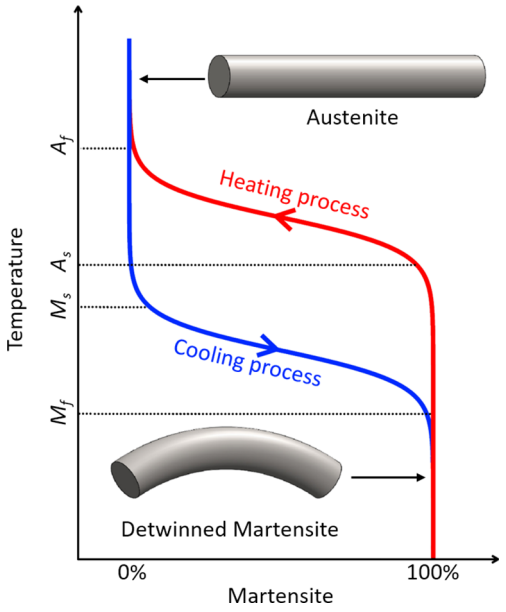

Figure 1. Phase conversion of two-way SMA and the critical temperatures during the phase conversion between austenite and martensite phases.

below M_f, it follows the A_s−A_f path as the temperature increases and the SMA changes state from a detwinned martensite to an austenite phase. Once the temperature of the SMA is between A_s and A_f, it retains its shape in that state even if the temperature subsequently decreases. The SMA will only change back to the martensite state if the temperature falls below M_s. Similarly, if the temperature falls below M_s and the SMA changes its state from an austenite phase back to the martensite phase, it follows the M_s−M_f path. The SMA will then remain in the state between M_s and M_f until the temperature is raised above A_s. This hysteresis enables it to monotonically change its overall shape with temperature and maintain a state corresponding to the peak temperature it experiences.

Input Impedance Reconfiguration of SMA-Based Antenna. The SMA used in this work is made of a conductive nickel−titanium alloy, commonly known as Nitinol. Therefore, by altering the shape of the antenna, the effective impedance can be altered by tuning the inductance and/or capacitance. As shown in Figure 2, a modified dipole antenna can be formed by

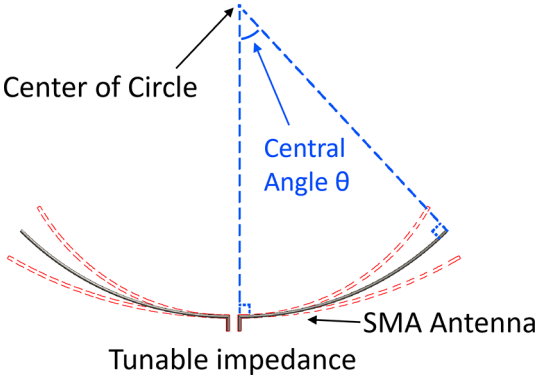

Figure 2. Modified dipole antenna with symmetrical bending arms.

symmetrically bending the two arms of the SMA wire. As it bends upward, the antenna on each side starts to form an arc of a circle. The central angle of the arc that an individual arm makes is marked as θ; a larger θ indicates more curvature of the SMA antenna.

In this experiment, a dipole antenna was implemented with an arm length of 0.49 times the wavelength, which has an input impedance of 65 + j3 ohm. The mapping relationship between the input impedance of the antenna and the central angle is obtained through the High-Frequency Structure Simulation (HFSS), as shown in Figure 3. As the central angle θ increases

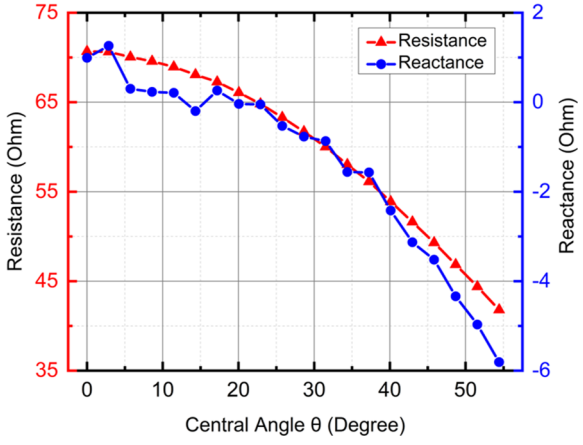

Figure 3. Dependence of antenna input impedance to the central angle θ of the modified dipole antenna.

from 0 to 55°, both the real and imaginary impedance of the antenna decrease. Since most antennas need to be matched to a standard 50-ohm port to connect to the rest of the RF circuit, our design can simply change the center angle to 43° for a near-perfect 50 − j3 ohm input impedance. If an antenna with a 60-ohm input impedance is needed to compensate for device mismatch, the central angle can be tuned to 31° to achieve the desired impedance. Thus, these modified antennas can be directly matched to a standard 50-ohm port or nonstandard port

https://doi.org/10.1021/acsomega.3c00550
ACS Omega 2023, 8, 14665−14671

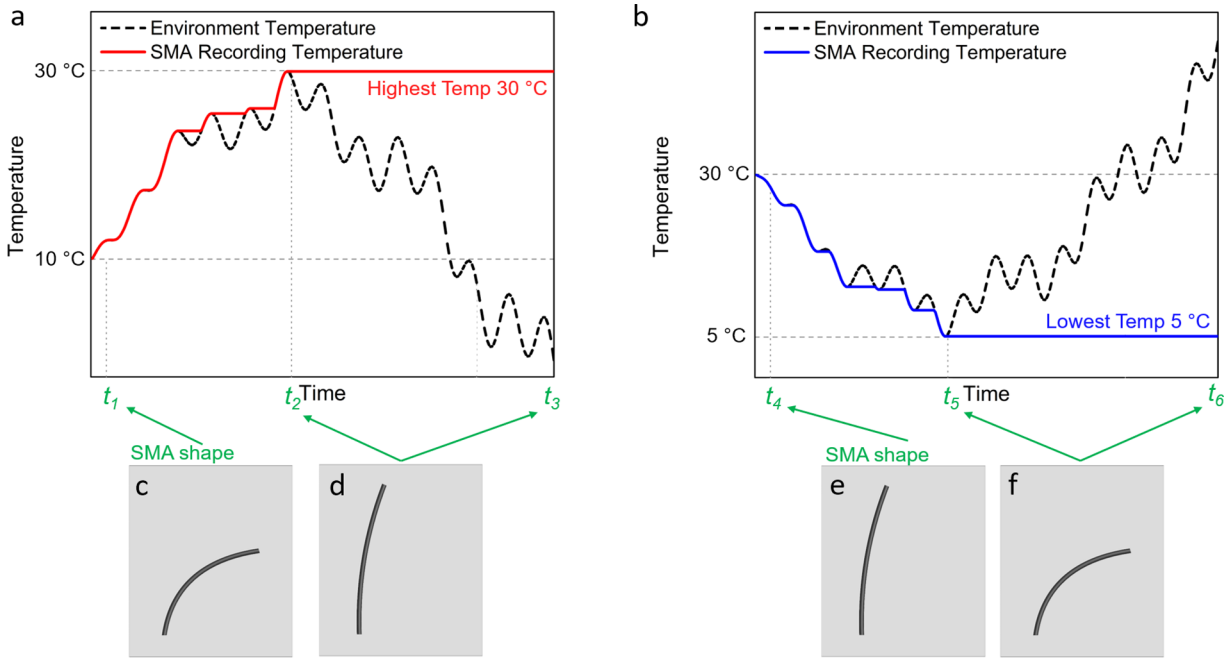

Figure 4. (a) Thermomechanical programming during the heating phase. The SMA's initial state is below temperature M_f. (b) Thermomechanical programming during the cooling phase. The SMA's initial state is above A_f. As the temperature increases from time t_1 to t_3, it (c) alters the shape and (d, e) tracks the highest temperature it experiences. Similarly, as the temperature decreases from time t_4 to t_6, it (f) alters the shape and (g, h) tracks the lowest temperature it experiences.

by central angle tuning without the need for impedance-matching circuits.

Principle of Two-Way Thermomechanical Programming of the SMA. A one-way SMA can change from a distorted shape to a predefined shape when heating, and it has only one predefined shape. However, a two-way SMA has one predefined shape at high temperatures and another predefined shape at low temperatures. A two-way SMA can change from its low-temperature predefined shape to the high-temperature predefined shape when heated, or it can convert from its high-temperature predefined shape to the low-temperature predefined shape when cooled.[26] For thermal state switching due to heating, the peak temperature that the SMA antenna experiences will determine the SMA configuration. As indicated in Figure 4(a), as the temperature of the SMA antenna goes from below M_f toward A_f, the SMA's shape changes in accordance with the temperature, as demonstrated in Figure 4(c) and (d), at times t_1 and t_2, respectively. If the temperature drops at some point, the SMA will no longer undergo any deformation and will hold its shape until the temperature rises again and reaches a new peak value. The SMA will remember the state corresponding to its highest experienced temperature, as shown at time t_3 in Figure 4(d). Similarly, the SMA starts with a high initial temperature above A_f for thermal state switching during cooling. As shown in Figure 4(b), as the temperature decreases, the SMA antenna will change shape to track the lowest experienced temperature in an analogous manner to what was discussed. The shape of the SMA at times t_4 and t_5 is shown in Figure 4(e) and (f), respectively. If the temperature increases at some point, the SMA will no longer undergo any deformation and will hold its shape until the temperature falls again, shown in Figure 4(f) at time t_6.

Regardless of how temperature is applied to the device, SMAs can be used to realize impedance tunable antennas. The high-temperature predefined shape at A_f and the low-temperature predefined shape at M_f dictate the range of input impedance tuning of the antenna. Through simulation, the relationship between the impedance and the temperature-dependent shape of the antenna can be identified, as shown in Figure 3. The thermomechanical memory of the SMA is monotonic as a function of peak temperature, thus allowing for continuous tuning of the input impedance of the SMA-based antenna using temperature.

SMA Antenna Fabrication. The input impedance tunable modified dipole antenna was implemented by adjusting the configuration through thermomechanical programming, as described below.

Step 1: Define the Input Impedance Range. The preferable input impedance range is between 40 ohm and 60 ohm for matching with standard ports. This reconfigurable impedance range allows the antenna to also match with nonstandard ports and to account for any mismatch errors from imperfect antenna geometry or parasitic capacitances. For example, when the antenna is implemented on a standard device with a 55-ohm output impedance, the antenna can be tuned close to 55 ohm to achieve the best power transfer efficiency. Thermomechanical programming will enable easy adjustment and tuning on account of any impedance mismatch.

Step 2: Obtain the Shape of the Antenna According to the Input Impedance Range in an EM Simulation. From the EM simulation, as shown in Figure 3, the shape can be programmed with input impedances of 40 ohm and 60 ohm through different choices of central angles. When the central angle of the antenna is 43°, it shows the characteristics of a standard 50-ohm antenna. To obtain a 60-ohm input impedance, a central angle of 32° is desired, while to achieve a 40-ohm input impedance, a central angle of 55° is needed. Since the input impedance decreases as the central angle increases, input impedance values between 40 ohm and 60 ohm are in the range of the antenna with a central angle between 32° and 55°.

https://doi.org/10.1021/acsomega.3c00550
ACS Omega 2023, 8, 14665−14671

Step 3: Training of the SMA-Based Antenna. From step 2, the two shapes of the antennas corresponding to input impedances of 40 ohm and 60 ohm are determined. An SMA antenna with these physical configurations will then need to be trained to undergo these precise deformations as a function of temperature. Thermomechanical training is required to obtain a two-way memory effect with proper temperature characteristics. The following processes, A and B, are required to train the two-way SMA with user-defined temperature behavior.[24]

Process A, forming a high-temperature predefined configuration: An SMA wire with 40 °C A_f is placed into a furnace at 300 °C and confined to the predefined austenite shape for 5 min. This process locks in the mechanical shape for high temperatures, to which the SMA will recover when exposed to heat.

Process B, forming a low-temperature predefined configuration: To form the low-temperature predefined configuration, a cold bath and a hot bath are used. The SMA wire is first coiled like a spring and placed in a cold bath below the M_f temperature for 5 min. The cold bath used is at 5 °C as shown in Figure 5(a).

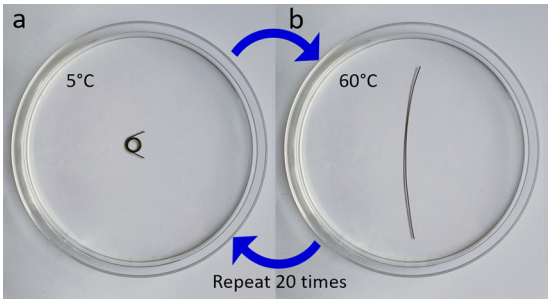

Figure 5. (a) Thermomechanical training of the low-temperature predefined configuration. (b) Thermomechanical training of the high-temperature predefined configuration.

The SMA is then placed in a hot bath at 60 °C. The hot bath is above the A_f temperature, and the SMA will recover to the high-temperature predefined shape as in Figure 5(b). After recovery, the SMA is coiled back to the spring shape and put into a cold bath again for another cycle. This process is repeated 20 times to lock in the respective configurations.

After training, the SMA wire begins to spontaneously change shape as temperature changes, curving to the direction in which it has been consistently deformed. It is important to note that the amount of the shape change on cooling will be significantly less than what was induced during the thermomechanical training steps mentioned above and needs to be calibrated before use. After process A and process B, a two-way SMA is formed. It will either change in accordance with temperature or lock to the peak value due to hysteresis.

Step 4: Characterization of the Central Angle θ versus Temperature and the Hysteresis Behavior. A dipole antenna was fabricated with its two arms composed of two trained SMA wires. Each wire is 75 mm in length and 0.5 mm in thickness. To characterize the temperature function and hysteresis, the SMA antenna was tested in an increasing-temperature setup and a decreasing-temperature setup, respectively. For the increasing-temperature test, the antenna was initially kept in a low-temperature environment below M_f (5 °C), so that it is in the low-temperature predefined shape. Then the temperature was gradually increased, and the SMA antenna's central angle was recorded as the temperature rose until it reached A_f and stopped changing. Similarly, the SMA antenna was tested in a decreasing-temperature setup. The measured results are shown in Figure 6.

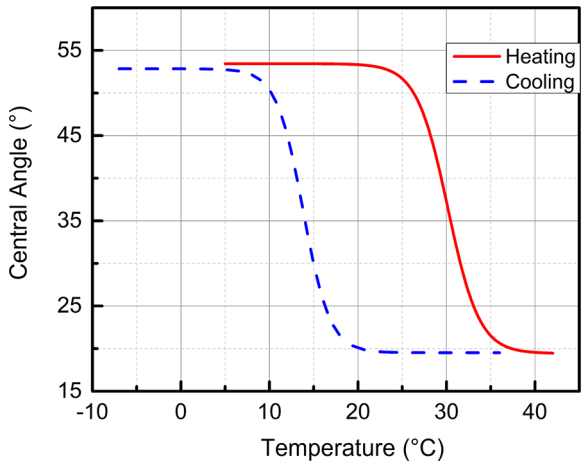

Figure 6. SMA with different central angles at different temperatures.

RESULTS

The reflected scattering S-parameters, S_{11}, of the SMA antenna at three different configurations were both simulated and measured. The three configurations have central angles of 32°, 43°, and 55°, corresponding to input impedance of 60, 50, and 40 ohm, respectively, as indicated in Figure 7(a), (b), and (c). The connected device port has a standard impedance of 50 ohm. The gains of the three configurations are 3, 2.5, and 2 dB, respectively, according to the simulation. As shown in Figure 7(d), (e), and (f), when the central angle is 43°, the SMA antenna shows the best performance due to the nearly perfect impedance matching between the standard port and the antenna. Both 32° and 55° show a worse matching for a 50-ohm port in both the simulation and experimental measurements. Similarly, the SMA-based antenna can be tuned to any nonstandard ports exhibiting a non-50 ohm impedance. For example, the antenna can be tuned with a 32° central angle to have its input impedance match 60 ohm. Simulation for antennas connected to both 50-ohm and 60-ohm ports for comparison was performed. In Figure 8(a), the blue dotted curve is the S_{11} simulation with the 60-ohm input impedance antenna connected to a 60-ohm output impedance port. In comparison, the red solid curve is the S_{11} simulation with the 60-ohm input impedance antenna connected to a 50-ohm output impedance port. The antenna can also be tuned with a 55° central angle to have an input impedance of 40 ohm. The antenna is connected to 40-ohm and 50-ohm ports for comparison in the simulation. In Figure 8(b), the blue dotted curve is the S_{11} simulation with the 40-ohm input impedance antenna connected to a 40-ohm output impedance port. In comparison, the red solid curve is the S_{11} simulation with the 40-ohm input impedance antenna connected to a 50-ohm output impedance port. As the results indicate, the antenna can be tuned to any non-50 ohm to achieve better matching to any nonstandard port.

DISCUSSION

Our simulation and experimental results show the ease of tuning an antenna impedance using a phase change material that can be programmed using temperature and does not rely on any

https://doi.org/10.1021/acsomega.3c00550
ACS Omega 2023, 8, 14665−14671

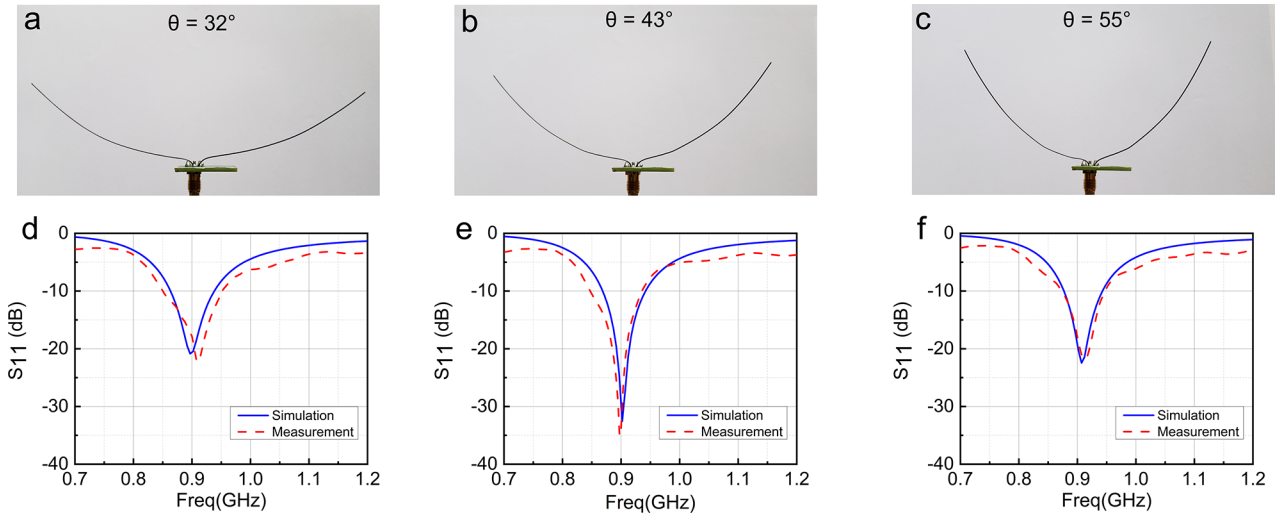

Figure 7. (a) Antenna with central angles of 32°, (b) 43°, and (c) 55°. (d) S_{11} response corresponding to 32°, (e) 43°, and (f) 55°.

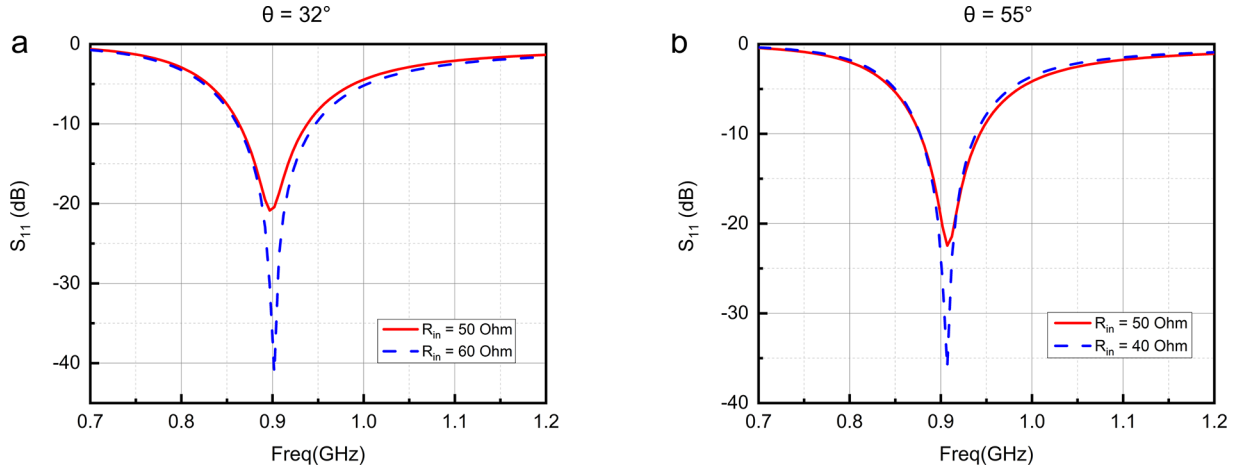

Figure 8. (a) S_{11} of SMA antenna at 32° used on a port with 50-ohm and 60-ohm impedance, respectively (b) S_{11} of SMA antenna at 55° used on a port with 50-ohm and 40-ohm impedance, respectively.

complex impedance-matching circuit networks. It is important to note that thermal-mechanical training gives the SMA a two-way memory. The memory recovery behavior is not perfect. In fact, recovery at high temperatures may be incomplete after the training cycle has been repeated several times compared to the original straight-line configuration due to the excessive deformation in the martensite phase. This is accounted for during calibration before use. It is important to point out that temperature is only used for programming the antenna. Also, both increasing and decreasing temperature profiles can be used to tune the antenna. Once programmed, the antenna locks in the configuration; thus, no further application of temperature is needed to maintain its shape. This is, however, only true if the environment temperature is in between its characteristic temperatures defined by the hysteresis in Figure 1. Only when the temperature drops below M_f or rises above A_f will the SMA antenna switch to the predefined shape. Once a specific antenna has been chosen and trained, its threshold points are fixed and can only be used in certain scenarios, which are determined by the antenna's operating temperature. The SMA antenna would not work if the operating temperature were beyond the hysteresis region since the SMA would change back to its predefined shape. As shown in Figure 6, if the antenna is working at −5 °C, it will not hold its shape since −5 °C is below M_f, and the SMA wire will return to a low-temperature predefined shape. To work in an environment with a temperature smaller than M_f or larger than A_f, one will need to switch to an SMA with a threshold temperature range close to the working temperature of the environment. While this paper focused on thermal training the input impedance of an antenna made with commercial SMA with thresholds around 30 °C, an SMA with a wider or different A_f and M_f range can be obtained by the specific training of the SMA and the SMA material selection.[28] Additionally, the shape change does not offer control of the real and imaginary parts individually. Future work will need to explore new and unique antenna shapes and configurations to train both the real and imaginary parts of the complex antenna impedance. The SMA could also be used in an antenna design with different temperature profiles to provide a more complex thermal programming pattern to tune the impedance of the antenna. Future work with thermal training can also be used to tune the gain, bandwidth, radiation pattern, beamwidth, and polarization.

CONCLUSION

In this work, a new paradigm to directly adjust the impedance of the antenna by using a temperature-dependent phase change

https://doi.org/10.1021/acsomega.3c00550
ACS Omega 2023, 8, 14665−14671

material was proposed. Thermal-mechanical programming is used to train the antenna response. Using the two-way memory effect and hysteresis of a shape memory alloy, the state (or shape) of the SMA-based antenna can be adjusted and maintained by setting the temperature. Different states (or shapes) of the SMA antenna correspond to different antenna impedances. Thus, the temperature can be used to change the shape and the impedance without the need for any additional circuit elements. Simulations and experiments were conducted to validate the design. The fabricated SMA antenna has an impedance range of 40 to 70 ohm and can work from below 10 to 35 °C. This phase change material-based programming provides a simple, easy-to-operate approach to achieving impedance matching for the antenna. By selecting SMA with different characteristics, it is possible to fabricate an SMA antenna to work in different temperature environments. This approach can be used in other applications where circuit function and performance are achieved through the hybrid integration of smart programmable matter with conventional electronics.

AUTHOR INFORMATION

Corresponding Author

Sameer R. Sonkusale − *Nano Lab, Department of Electrical and Computer Engineering, Tufts University, Medford, Massachusetts 02155, United States;* orcid.org/0000-0003-3579-910X; Email: sameer@ece.tufts.edu

Authors

Wei Wang − *Nano Lab, Department of Electrical and Computer Engineering, Tufts University, Medford, Massachusetts 02155, United States;* Present Address: Analog Devices, 950 Chapel Hills Dr, Colorado Springs, Colorado 80920, United States

Wenxin Zeng − *Nano Lab, Department of Electrical and Computer Engineering, Tufts University, Medford, Massachusetts 02155, United States*

Complete contact information is available at: https://pubs.acs.org/10.1021/acsomega.3c00550

Notes

The authors declare no competing financial interest.

ACKNOWLEDGMENTS

The authors thank funding from the U.S. National Science Foundation (NSF) through Grant numbers 1935555, 1951104, and 1808912. The authors thank Ravi Durbha for his advice on the antenna design and simulation.

REFERENCES

(1) Alam, M. S.; Abbosh, A. A Compact Reconfigurable Antenna With Wide Tunable Frequency and 360° Beam Scanning. *IEEE Antennas and Wireless Propagation Letters* **2019**, *18*, 4−8.

(2) Yashchyshyn, Y.; Derzakowski, K.; Bajurko, P. R.; Marczewski, J.; Kozłowski, S. Time-Modulated Reconfigurable Antenna Based on Integrated S-PIN Diodes for mm-Wave Communication Systems. *IEEE Transactions on Antennas and Propagation* **2015**, *63*, 4121−4131.

(3) Bai, Y.-Y.; Xiao, S.; Liu, C.; Shuai, X.; Wang, B.-Z. Design of Pattern Reconfigurable Antennas Based on a Two-Element Dipole Array Model. *IEEE Transactions on Antennas and Propagation* **2013**, *61*, 4867−4871.

(4) Xu, Y.; Tian, Y.; Zhang, B.; Duan, J.; Yan, L. A novel RF MEMS switch on frequency reconfigurable antenna application. *Microsystem Technologies* **2018**, *24*, 3833−3841.

(5) Rao, K. S.; Naveena, P.; Sravani, K. G. Materials Impact on the Performance Analysis and Optimization of RF MEMS Switch for 5G Reconfigurable Antenna. *Transactions on Electrical and Electronic Materials* **2019**, *20*, 315−327.

(6) Wang, W.; Sadeqi, A.; Nejad, H. R.; Sonkusale, S. Cost-Effective Wireless Sensors for Detection of Package Opening and Tampering. *IEEE Access* **2020**, *8*, 117122−117132.

(7) Wang, W.; Sadeqi, A.; Sonkusale, S. All-Around Package Security Using Radio Frequency Identification Threads. *2018 IEEE Sensors* **2018**, 1−4.

(8) He, H.; Chen, X.; Mehmood, A.; Raivio, L.; Huttunen, H.; Raumonen, P.; Virkki, J. ClothFace: ABatteryless RFID-Based Textile Platform for Handwriting Recognition. *Sensors* **2020**, *20*, 4878.

(9) Miozzi, C.; Amato, F.; Marrocco, G. Performance and Durability of Thread Antennas as Stretchable Epidermal UHF RFID Tags. *IEEE Journal of Radio Frequency Identification* **2020**, *4*, 398−405.

(10) Asci, C.; Wang, W.; Sonkusale, S. Security Monitoring System Using Magnetically-Activated RFID Tags. *2020 IEEE Sensors* **2020**, 1−4.

(11) Wang, W.; Asci, C.; Zeng, W.; Sonkusale, S. Zero-power screen printed flexible RFID sensors for Smart Home. *Journal of Ambient Intelligence and Humanized Computing* **2023**, *14*, 3995−4004.

(12) Wang, Y.; Yan, C.; Cheng, S.; Xu, Z.; Sun, X.; Xu, Y.; Chen, J.-j.; Jiang, Z.; Liang, K.; Feng, Z. Flexible RFID Tag Metal Antenna on Paper-Based Substrate by Inkjet Printing Technology. *Adv. Funct. Mater.* **2019**, *29*, 1902579.

(13) Wang, W.; Owyeung, R.; Sadeqi, A.; Sonkusale, S. Single Event Recording of Temperature and Tilt Using Liquid Metal With RFID Tags. *IEEE Sensors Journal* **2020**, *20*, 3249−3256.

(14) Yang, X.; Liu, Y.; Lei, H.; Jia, Y.; Zhu, P.; Zhou, Z. A Radiation Pattern Reconfigurable Fabry-Pérot Antenna Based on Liquid Metal. *IEEE Transactions on Antennas and Propagation* **2020**, *68*, 7658−7663.

(15) Paracha, K. N.; Butt, A. D.; Alghamdi, A. S.; Babale, S. A.; Soh, P. J. Liquid Metal Antennas: Materials, Fabrication and Applications. *Sensors* **2020**, *20*, 177.

(16) Tawk, Y. Physically Controlled CubeSat Antennas With an Adaptive Frequency Operation. *IEEE Antennas and Wireless Propagation Letters* **2019**, *18*, 1892−1896.

(17) Islam, S. N.; Kumar, M.; Sen, G.; Das, S. Design of a compact triple band antenna with independent frequency tuning for MIMO applications. *International Journal of RF and Microwave Computer-Aided Engineering* **2019**, *29*, e21620.

(18) Zainarry, S. N. M.; Nguyen-Trong, N.; Fumeaux, C. A Frequency- and Pattern-Reconfigurable Two-Element Array Antenna. *IEEE Antennas and Wireless Propagation Letters* **2018**, *17*, 617−620.

(19) Sumana, L.; Sundarsingh, E. F.; Priyadharshini, S. Shape Memory Alloy-Based Frequency Reconfigurable Ultrawideband Antenna for Cognitive Radio Systems. *IEEE Transactions on Components, Packaging and Manufacturing Technology* **2021**, *11*, 3−10.

(20) Boukarkar, A.; Lin, X. Q.; Jiang, Y.; Chen, Y. J.; Nie, L. Y.; Mei, P. Compact mechanically frequency and pattern reconfigurable patch antenna. *IET Microwaves, Antennas & Propagation* **2018**, *12*, 1864−1869.

(21) Sanchez-Olivares, P.; Masa-Campos, J. L. Mechanically Reconfigurable Conformal Array Antenna Fed by Radial Waveguide Divider With Tuning Screws. *IEEE Transactions on Antennas and Propagation* **2017**, *65*, 4886−4890.

(22) Zhang, X. G.; Jiang, W. X.; Tian, H. W.; Wang, Z. X.; Wang, Q.; Cui, T. J. Pattern-Reconfigurable Planar Array Antenna Characterized by Digital Coding Method. *IEEE Transactions on Antennas and Propagation* **2020**, *68*, 1170−1175.

(23) Kowalewski, J.; Mahler, T.; Reichardt, L.; Zwick, T. Shape Memory Alloy (SMA)-Based Pattern-Reconfigurable Antenna. *IEEE Antennas and Wireless Propagation Letters* **2013**, *12*, 1598−1601.

(24) Wang, W.; Zeng, W.; Ruan, W.; Miller, E.; Sonkusale, S. Thermo-Mechanically Trained Shape Memory Alloy for Temperature Recording With Visual Readout. *IEEE Sensors Letters* **2021**, *5*, 1−4.

(25) Wang, W.; Zeng, W.; Sonkusale, S. Battery-Free Shape Memory Alloy Antennas for Detection and Recording of Peak Temperature Activity. *Crystals* **2022**, *12*, 86.
(26) Zeng, W.; Wang, W.; Sonkusale, S. Temperature Sensing Shape Morphing Antenna (ShMoA). *Micromachines* **2022**, *13*, 1673.
(27) Mohd Jani, J.; Leary, M.; Subic, A.; Gibson, M. A. A review of shape memory alloy research, applications and opportunities. *Materials and Design* **2014**, *56*, 1078−1113.
(28) Jiang, J.; Cui, L.; Zheng, Y.; Jiang, D.; Liu, Z.; Zhao, K. Narrow hysteresis behavior of TiNi shape memory alloy constrained by NbTi matrix during incomplete transformation. *Materials Science and Engineering: A* **2012**, *536*, 33−36.

https://doi.org/10.1021/acsomega.3c00550
ACS Omega 2023, 8, 14665−14671